Human Pathology (2007) **38**, 1454–1462

ELSEVIER

Human PATHOLOGY

www.elsevier.com/locate/humpath

Original contribution

Automated immunofluorescence analysis defines microvessel area as a prognostic parameter in clear cell renal cell cancer☆

Kirsten D. Mertz MD[a,b,d], Francesca Demichelis PhD[a,b], Robert Kim [a], Peter Schraml PhD[d], Martina Storz [d], Pierre-André Diener MD[e], Holger Moch MD[d,*], Mark A. Rubin MD[a,b,c,*]

[a] *Department of Pathology, Brigham and Women's Hospital, Boston, MA 02115, USA*
[b] *Harvard Medical School, Boston, MA 02115, USA*
[c] *Dana-Farber Harvard Cancer Center, Boston, MA 02115, USA*
[d] *Institute of Surgical Pathology, University Hospital Zurich, 8091 Zurich, Switzerland*
[e] *Institute of Pathology, Hospital St. Gallen, CH-9007 St. Gallen, Switzerland*

Received 27 January 2007; revised 11 May 2007; accepted 16 May 2007

Keywords:
Clear cell renal cell cancer;
Microvessel density (MVD);
Microvessel area (MVA);
Automated quantitative analysis (AQUA);
Prognosis

Summary Microvessel density (MVD) has been reported to have prognostic relevance for clear cell renal cell carcinoma (ccRCC). However, this finding is controversial because of the difficulty of MVD evaluation in this complex vascularized tumor type. The present study evaluates the use of an automated quantitative analysis (AQUA) system for objective and reproducible determination of tumor vascularization in clear cell renal cell carcinoma (ccRCC). The AQUA system was applied to tissue microarrays with 284 primary ccRCC tumors. To determine angiogenesis in ccRCC, we created an epithelial/stromal mask consisting of CD10, epithelial membrane antigen, and vimentin to distinguish epithelial tumor cells from CD34-positive endothelial cells. Using immunofluorescence and computer-aided quantification of CD34 expression, we measured the relative microvessel area (MVA) and compared the MVA to the manually counted MVD. The MVA determined by AQUA in a test set with 209 ccRCCs ranged from 0% to 30.3% (mean ± SD, 10.1% ± 6.3%). The manually determined MVD ranged from 6 to 987 vessels/mm^2 (416.8 ± 252.8 vessels/mm^2). MVA and MVD were significantly correlated ($P < .001$). A larger MVA was associated with histologic grade ($P < .001$), tumor stage ($P = .008$), presence of metastasis ($P = .005$), presence of sarcomatoid areas ($P < .001$), and tumor-specific survival ($P < .001$). Using MVA as defined in the test set, all associations with clinical and pathologic parameters were confirmed in a second independent validation set. MVA determination by AQUA is an objective and reliable method to quantify tumor vascularization in ccRCC. A large MVA correlates with a high MVD and is associated with better patient prognosis.

☆ This work was supported by the NIH NCI P50 CA090381Prostate SPORE at the Dana-Farber/Harvard Cancer Center (MAR), the Swiss National Science Foundation 323880-103145/1 (HM), and the Swiss Foundation for Medical-Biological Grants SSMBS, SNF no. 1168 (KM).

* Corresponding authors. Holger Moch is to be contacted at Institute of Surgical Pathology, University Hospital Zurich, Schmelzbergstrasse 12, CH-8091 Zurich, Switzerland. Mark A. Rubin, Department of Pathology, Brigham and Women's Hospital, Harvard Medical School, Boston, MA 02115-6110, USA.
E-mail addresses: holger.moch@usz.ch (H. Moch), marubin@partners.org (M. A. Rubin).

0046-8177/$ – see front matter © 2007 Published by Elsevier Inc.
doi:10.1016/j.humpath.2007.05.017

1. Introduction

Clear cell renal cell cancer (ccRCC) is the most common subtype of renal cell cancer (RCC). The *VHL* gene is inactivated in ccRCC of patients with the von Hippel-Lindau (VHL) syndrome and in most sporadic ccRCCs. Inactivation of the VHL tumor suppressor protein (pVHL) through mutation or inhibition of expression leads to constitutive hypoxia-inducible transcription factor (HIF) activation, an event that is believed to contribute to the regulation of vascular endothelial growth factor (VEGF). VEGF is an angiogenetic factor that may be involved in tumor growth and metastasis. It is postulated that ccRCC is therefore characterized by rich neovascularization and an often prominent vascular network around tumor cells. They often metastasize via the vascular route, suggesting tumor angiogenesis as an important parameter for ccRCC progression.

Microvessel density (MVD) defined as the number of small vessels for a given tumor area is used as a measure of angiogenesis in solid tumors [1]. MVD is frequently determined by using a method introduced by Weidner [1], which defines rules for reproducible microvessel counting. For several carcinomas including breast [2], prostate [3], bladder [4], colon [5], stomach [6], ovary [7], and melanoma [8], angiogenesis is independently associated with metastasis and lower disease-specific survival.

In contrast, in ccRCC the relationship between vascularity as measured by MVD and prognosis are conflicting. An association between high MVD and poor prognosis was reported by Joo et al [9] and Fukata et al [10]. Other groups have observed an association between high MVD and better prognosis [11-15], whereas some groups failed to confirm the association between MVD and prognosis [16,17]. These discrepancies may be attributable to interobserver variability in precisely determining MVD in ccRCC [13,18]. The method used by Weidner is semiquantitative, depending on the experience of the pathologist and on poorly controlled variables, including quality of endothelial cell immunohistochemistry. Furthermore, the method may not account for the complexity of microvessel architecture in ccRCC with its extremely high degree of vascular branching and irregularity.

Recently, an automated quantitative analysis (AQUA) system has been introduced by Camp and colleagues [19,20]. The fluorescence-based AQUA system automatically measures and localizes disease-specific variations in protein expression within tissues. It is objective and reproducible, with features lacking in manual biomarker evaluation. AQUA can be applied to standard tissue samples or tissue microarrays (TMAs), allowing automated high-throughput quantification of biomarkers [21].

Consequently, in this study we evaluate the use of the AQUA system to measure vascularization in ccRCC. In contrast to MVD, which is determined by manual counting according to Weidner [1], we established the area of microvessels (microvessel area [MVA]) as a new parameter for the measurement of vascularization by AQUA. We developed a computer-aided approach to determine angiogenesis in primary ccRCCs by using an antibody against the endothelial marker CD34 and defined a ccRCC-specific epithelial/stromal mask with epithelial membrane antigen (EMA), CD10, and vimentin. The results were compared with prognostic parameters of ccRCC (tumor grade, stage, size, metastasis, presence of necrosis) and cancer-specific survival. The AQUA approach allowed for fast, objective, straightforward, and highly reproducible measurement of tumor vascularity in a high-throughput setting. An association between a large area of microvessels and better patient prognosis was confirmed with TMAs.

2. Material and methods

2.1. Patients and TMAs

RCC patients were identified from the files of the Institute for Surgical Pathology, Department of Pathology of the University Hospital Zurich, Switzerland, and from the Institute for Pathology, Kantonsspital St. Gallen, Switzerland. All samples were collected from patients, who gave their consent, with prior institutional review board approval at each respective institution. All RCCs were histologically reevaluated by a pathologist (HM) and selected for the study on the basis of hematoxylin and eosin-stained tissue sections. For both the Zurich and the St. Gallen cohorts, an RCC TMA was constructed as previously described [22]. Tumors were staged according to the TNM staging system and histologically classified according to the World Health Organization classification [23]. Tumor-specific survival data were obtained by reviewing the hospital records and by direct communication with the attending physicians.

The Zurich TMA included 356 renal tumors and the St. Gallen TMA 200 renal tumors. For further analysis, only ccRCCs with clinical follow-up information were selected. There were 209 ccRCC tumors from Zurich and 75 ccRCC tumors from St. Gallen. The combined clinical and pathologic parameters of both patient cohorts are summarized in Table 1. There were 189 men and 95 women. The median age was 65 years (range, 22-88 years). There were 6 Fuhrman grade I, 85 Fuhrman grade II, 123 Fuhrman grade III, and 70 Fuhrman grade IV tumors. One hundred and sixteen tumors were stage pT1, 28 were pT2, 133 were pT3, and 7 were pT4. Thirty-nine patients (21.7%) had distant metastases at the time of surgery. The mean follow-up of patients was 52 months (range, 1-179 months). There were 116 cancer-related deaths.

2.2. Automated image acquisition and analysis

The automated image acquisition and analysis system (AQUA) has been described elsewhere [19-21]. In brief, multiple, monochromatic, high-resolution (2048 × 2048

Table 1 Clinicopathologic characteristics of patients and tumors

Clinical parameters	Hospital cohorts	
	Zurich patients (%)	St Gallen patients (%)
Events		
Censor	120 (57.4)	48 (64.0)
Death	89 (42.6)	27 (36.0)
Fuhrman grade		
1	3 (1.4)	3 (4.0)
2	57 (27.3)	28 (37.3)
3	89 (42.6)	34 (45.3)
4	60 (28.7)	10 (13.3)
pT stage		
1	83 (39.7)	33 (44.0)
2	16 (7.7)	12 (16.0)
3	106 (50.7)	27 (36.0)
4	4 (1.9)	3 (4.0)
Sarcomatoid features		
Absent	148 (70.8)	NA
Present	61 (29.2)	NA
Necrosis		
Absent	133 (63.6)	60 (82.2)
Present	76 (36.4)	13 (17.8)
Nodal status		
Absent	79 (87.8)	49 (87.5)
Present	11 (12.2)	7 (12.5)
Metastatic status		
Absent	75 (71.4)	66 (88.0)
Present	30 (28.6)	9 (12.0)
Lymphocytic infiltrate		
Absent	38 (18.2)	NA
Present	171 (81.8)	NA
Size (cm^3)		
≤163	68 (56.2)	17 (34.7)
164+	53 (43.8)	32 (65.3)
Sex		
Women	74 (35.4)	21 (28.0)
Men	135 (64.6)	54 (72.0)
Age (y)		
≤65	105 (50.2)	45 (60.0)
66+	104 (49.8)	30 (40.0)

pixels) images are obtained from each TMA spot with an Olympus BX51RF epifluorescence microscope (Olympus, Melville, NY) set up with a series of user modifications including an automated Prior microscope stage with digital image acquisition (Optronics QuantiFIRE, Goleta, CA) driven by custom program and macro-based interfaces with proprietary software (HistoRX Inc, New Haven, CT), through a 20× Plan Apo objective.

2.3. Definition of the MVA

To estimate the extent of angiogenesis in a solid tumor by AQUA, we defined the MVA in a given tumor. The CD34-positive compartment is consistent with endothelial cells in small vessels [24]. Areas of CD34-positive endothelial cells are distinguished from epithelial and stromal elements by creating a mask from CD10/EMA/vimentin signals. ccRCC tumors react positively for at least 1 of the antibodies against CD10, EMA, and vimentin [22,25,26]. Because vimentin also detects all mesenchymal cells in RCC, the CD10/EMA/vimentin compartment is equivalent to all epithelial and stromal cells in the 0.6-mm diameter TMA spot. AQUA was used to quantify the areas positive for CD34 staining within areas of EMA, CD10, and vimentin positivity. The MVA was defined as the area of CD34 staining normalized to the area of tissue represented by the epithelial/stromal mask (MVA = CD34 area / (CD10 area + EMA area + vimentin area)). CD34-positive areas outside the epithelial/stromal mask were not used for the calculation of MVA.

2.4. Immunofluorescence

TMA sections were freshly cut and stained. After pressure cooker pretreatment in citrate buffer (0.01 ml/L, pH 6.0), TMA sections were blocked with 0.3% BSA in TBS for 1 hour at room temperature, followed by incubation with a primary mouse monoclonal antibody against the endothelial marker CD34 (clone QBEnd 10, 1:800; Dako, Carpinteria, CA) overnight at 4°C. CD34 staining was visualized by incubation with the antimouse Envision kit (horseradish peroxidase [HRP] labeled polymer; Dako) for 1 hour at room temperature and Cy-5 tyramide (1:50) in amplification diluent for 10 minutes. In the next step, the same sections were incubated with a mixture of the following primary antibodies for 2 hours at room temperature: mouse monoclonal anti-CD10 (Novocastra, clone 56C6, 1:80), mouse monoclonal antihuman EMA (Dako; clone E29, 1:800), mouse monoclonal antihuman vimentin (Dako; clone Vim 3B4, 1:800). All antibodies were titrated to optimize signal to noise ratio. A secondary antibody, antimouse Alexa Fluor 555 (1:200), was then used to detect the primary antibody mixture. Each section was counterstained by using a premixed solution of 4,6-diamidino-2-phenylindole (DAPI) and antifade mounting media (ProLong Gold antifade reagent with DAPI; Invitrogen Corporation, Eugene, OR). DAPI was added to visualize nuclei. CD34 was visualized with a fluorescent chromogen (Cy-5-tyramide; NEN Life Science Products, Boston, MA) which, like diaminobenzidine, is activated by HRP and results in the deposition of numerous covalently associated Cy-5 dyes immediately adjacent to the HRP-conjugated secondary antibody. As previously described, Cy-5 (red) was used because its emission peak is well outside the green-orange spectrum of tissue autofluorescence [19,20].

2.5. Statistical analysis

To optimize the computerized analysis of MVA by AQUA, we used the Zurich cohort as a training set

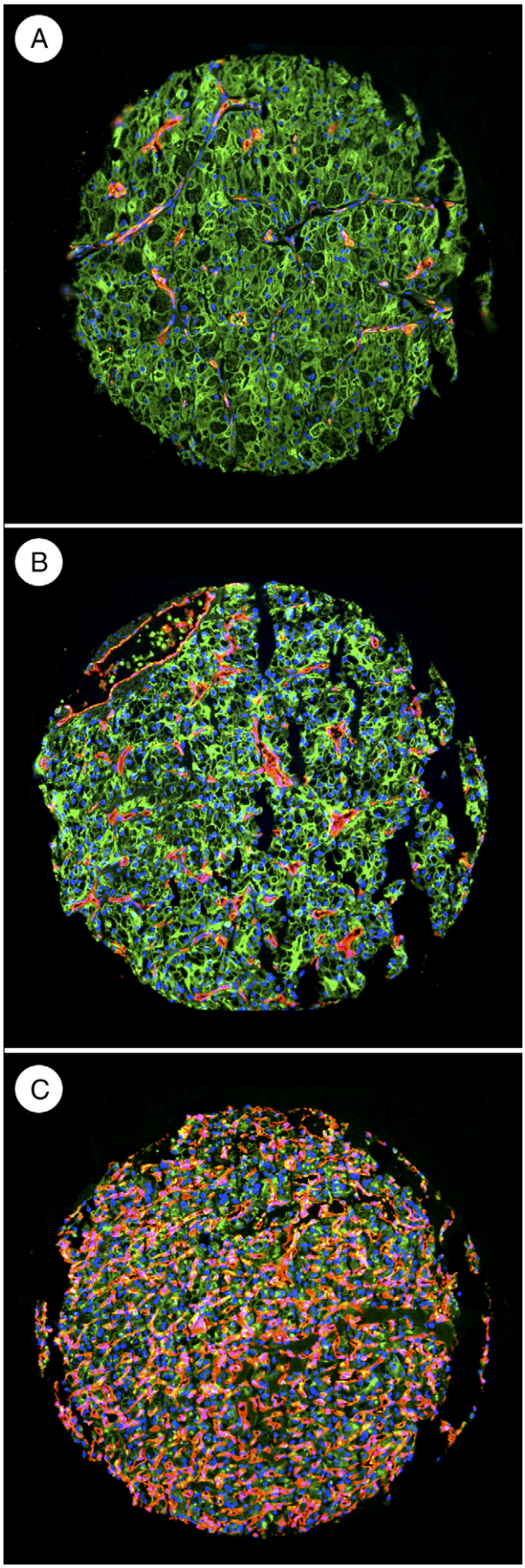

(209 cases) and the St. Gallen cohort as a test set (75 cases). The Zurich training set was used to determine the optimal cutoff points to separate low, medium, and high MVA in ccRCC and to compare the MVA with the manually counted MVD. In a second step, the cutoff points were validated using the St. Gallen test set. All clinical and pathologic parameters were explored for their associations with MVA. Kaplan-Meier analysis was used to generate survival curves with respect to cancer-specific death for MVA and the pathology parameters. Survival time was calculated from date of nephrectomy to date of death or to date of last clinical follow-up. The log-rank test was used to evaluate statistical significance of associations. Cox proportional hazard regression analysis for survival was used for univariate and multivariate analysis (backward stepwise by Wald statistics). The association of MVA with categorized clinical and pathologic parameters was determined with analysis of variance posthoc Scheffé analysis and independent *t* test analysis. All statistics were performed by using SPSS 13.0 for Windows (SPSS Inc, Chicago, IL) with a significance level of 0.05.

3. Results

3.1. MVA and MVD

Immunofluorescent staining for the endothelial marker CD34 revealed heterogeneously distributed microvessels in ccRCC with an extremely high degree of vascular branching and irregularities. Representative CD34-stained sections of ccRCCs with small, medium, and large MVA values are shown in Fig. 1.

The MVA as determined by AQUA ranged from 0% to 30.3% (mean ± SD, 10.1% ± 6.3%). A large MVA (>10%) was associated with histologic grade ($P < .001$), tumor stage ($P = .008$), presence of metastasis ($P = .005$), and presence of sarcomatoid areas ($P < .001$). Tumors from patients with metastatic disease (n = 39) had a significantly smaller MVA as compared to patients with clinically localized disease (n = 141), with median AQUA scores of 8.2% ± 5.4% and 11.2% ± 7.0%, respectively ($P = .005$). In the presence of sarcomatoid features, necrosis, lymphocytic infiltrates, and positive regional lymph nodes, MVA was significantly decreased (Table 2).

Fig. 1 Immunofluorescence analysis of representative ccRCC cases. AQUA of MVA required developing a method for identifying the tumor by creating a tumor mask. The ccRCC tumor mask used a combination of anti-CD10, anti-EMA, and anti-vimentin antibodies (green) because most tumors expressed at least 1 of these proteins. The area of microvessels could then be determined within this tumor mask by using an anti-CD34 antibody (red). Nuclei were counterstained with DAPI (blue). Examples of small (A), medium (B), and large MVA (C).

For the Zurich cohort, MVD was also manually counted by a pathologist (HM) using the method described by Weidner [1]. The manually determined MVD ranged from 6 to 987 vessels/mm^2, the mean MVD was 416.8 ± 252.8 vessels/mm^2 (mean ± SD). There was a significant correlation between MVA and MVD ($P < .001$) (Fig. 2).

3.2. Patient survival

All established prognostic parameters, including presence of metastasis, tumor stage, nuclear grade, presence of sarcomatoid differentiation, presence of necrosis, and brisk lymphocytic infiltration, were associated with prognosis in the training and test set. The mean percentage of microvessels for all 284 tumors was 10.1%. By using MVA as a continuous variable, we did not find a statistically significant correlation between MVA and patient survival. Using the Zurich cohort as a training set, we identified 2 optimal cutoff values for MVA, 4% and 14% MVA. These values correspond to the mean of the MVA distribution in the training cohort ± 1 SD, respectively. Accordingly, we subdivided tumors into large (>14%), medium (≤14% and >4%), and small (≤4%) MVA categories. When these categories were used, survival rates of patients with large MVA were significantly better than that of patients with small MVA ($P = .004$). Patients with medium MVA showed medium survival rates, as shown in Fig. 3A.

Table 2 MVA according to nuclear grade, tumor stage, sarcomatoid features (for Zurich cohort only, 209 patients), necrosis, lymphocytic infiltration (for Zurich cohort only, 209 patients), and metastatic status in 284 patients with ccRCC

Clinical parameters	No. of cases	% MVA (SD)	*P*
Fuhrman grade			
1 + 2	91	12.95 (5.7)	<.001
3 + 4	193	8.7 (6.2)	
Stage			
pT1 + pT2	144	11.1 (6.1)	.008
pT3 + pT4	140	9.1 (6.4)	
Sarcomatoid features			
Absent	148	10.7 (4.8)	<.001
Present	61	5.7 (4.9)	
Necrosis			
Absent	193	11.9 (6.0)	<.001
Present	89	6.1 (5.0)	
Lymphocytic infiltration			
Absent	38	12.2 (4.5)	<.001
Present	171	8.5 (5.2)	
Nodal disease			
Absent	128	10.9 (6.7)	<.001
Present	18	4.8 (4.3)	
Metastasis			
Absent	141	11.2 (7.0)	.005
Present	39	8.2 (5.4)	

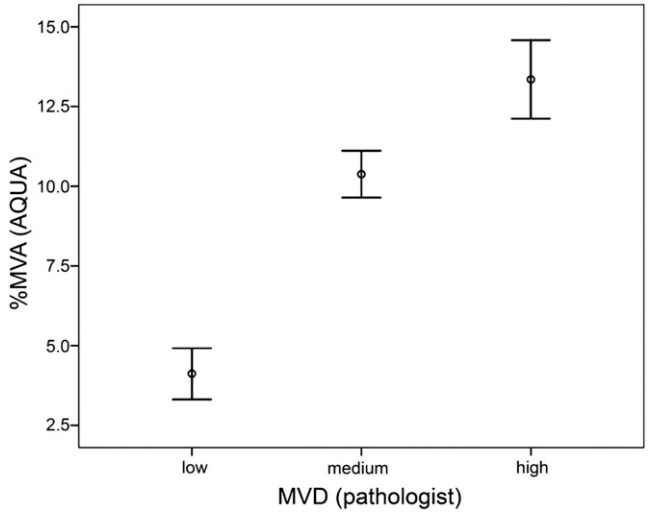

Fig. 2 Correlation between MVD (manually counted) and MVA (AQUA) in the training cohort. For the Zurich cohort, MVD was manually quantified by an experienced pathologist (HM) and subdivided in cases with low (n = 62), medium (n = 97), and high (n = 50) MVD; MVA was automatically and objectively determined by AQUA. Comparison of both approaches revealed that the automated MVA determination correlated with manual counting of microvessels by an expert ($P < .001$).

The MVA categories defined in the training cohort were applied to the St. Gallen test cohort. Also in this cohort, statistically significant survival differences were observed ($P = .03$) (Fig. 3B). Fig. 3C shows the survival curves for both cohorts together ($P < .001$). Regression analysis of MVA in the combined cohort showed relative risk (RR) for low MVA equal to 2.82 (95% confidence interval [CI], 1.71-4.65; $P < .001$).

Table 3 reports the RRs, as obtained by Cox proportional hazards regression analysis, at the univariate and multivariate level. Multivariate analysis included all variables significantly associated with patient survival in univariate analysis. Metastatic status (RR, 6.33; 95% CI, 2.79-14.38; $P < .001$) and sarcomatoid features (RR, 2.34; 95% CI, 1.13-4.88; $P = .023$) emerged as independent prognostic factors for cancer-specific survival at a multivariate level (Table 3). MVA was found not to be an independent prognostic parameter.

4. Discussion

Tumor growth is dependent on angiogenesis. There is evidence to suggest an association between tumor vascularity and patient survival in a variety of malignant neoplasms. An increased MVD has been associated with early progression in a number of tumors [2-8]. Such an association is likely due to increased nutrient transfer in hypervascular tumors, promoting the establishment of

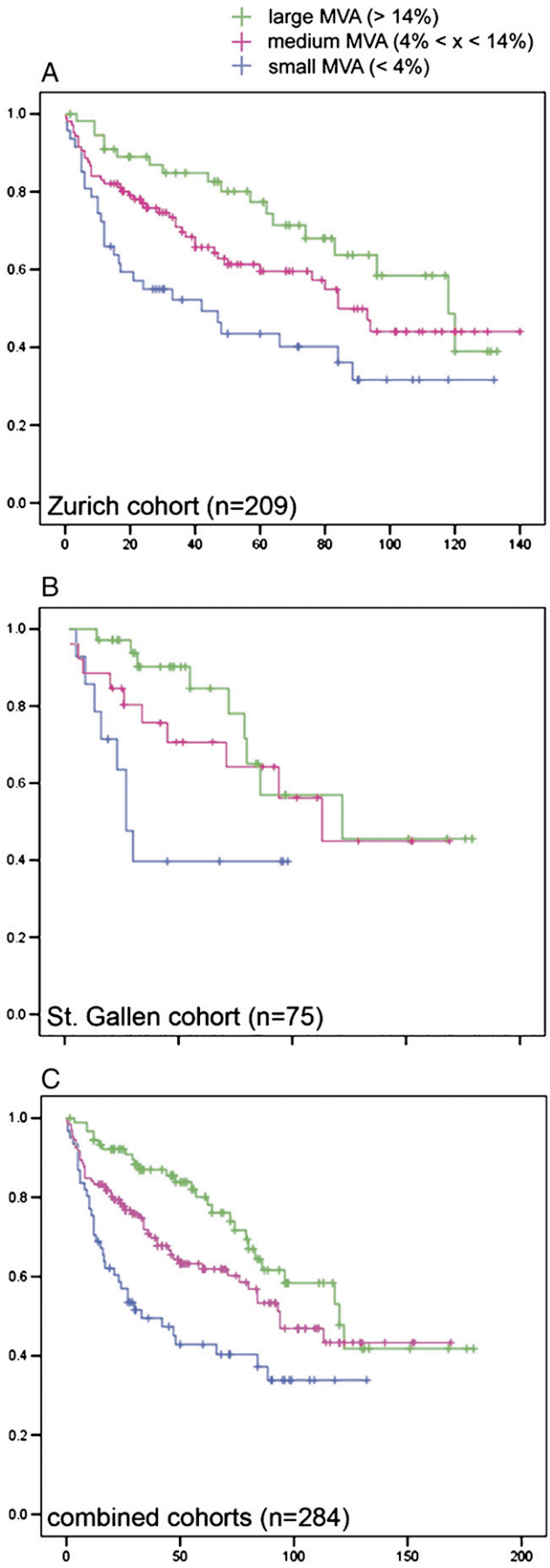

Table 3 Cancer-specific death regression analysis for the combined ccRCC cohorts from Zurich and St. Gallen (n = 284). Univariate and multivariate analyses (ns, not significant)

Variables	Univariate			Multivariate		
	95% CI	RR	*P*	95% CI	RR	*P*
Fuhrman grade						
3/4 (REF 1/2)	1.71-4.33	2.72	<.001			ns
Stage						
pT3/4 (REF pT1/2)	2.24-5.00	3.35	<.001			ns
MVA (%)						
Medium (REF Large)	1.01-2.53	1.59	.049			ns
Small (REF Large)	1.71-4.65	2.82	<.001			ns
Sarcomatoid features						
Present (REF Absent)	1.36-3.15	2.07	.001	1.13-4.88	2.34	.023
Necrosis						
Present (REF Absent)	1.94-4.03	2.80	<.001			ns
Lymphocytic infiltration						
Present (REF Absent)	1.24-4.93	2.47	.010			ns
Nodal status						
pN1 present (REF pN0)	2.47-8.10	4.47	<.001			ns
Metastatic status						
cM1 (REF cM0)	2.93-7.68	4.75	<.001	2.79-14.38	6.33	<.001

more rapidly proliferating tumor cells. Indeed, it has been shown for various malignancies that more actively proliferating tumors have a greater MVD [27]. Higher

Fig. 3 Large MVA is correlated to better patient survival. To subdivide our ccRCC specimens in cases with large, medium, and small MVA, we determined 2 optimal cutoff values: 4% and 14% MVA. These values correspond to the mean of the MVA distribution in the training cohort ± 1 SD, respectively. Cases with an MVA of more than 14% were considered to have a large MVA, cases with an MVA of 4% or lower have a small MVA, and intermediate cases have an MVA between 4% and 14%. By using this definition, we found that the survival rate of patients with large MVA was significantly higher than that of patients with small MVA in the Zurich cohort (A) ($P = .004$), the St. Gallen cohort (B) ($P = .03$), and the combined cohorts (C) ($P < .001$).

vascular density within a tumor also provides increased opportunity for vascular infiltration by malignant cells, leading to metastatic dissemination via the vascular route or via lymphatics associated with the developing vascular network [28].

In contrast, in ccRCC, which is among the most vascularized of all solid tumors, the prognostic value of MVD as assessed by different methods and staining evaluations is unclear. Several angiogenesis assays are commonly used, but objective assessment of new vascular growth is difficult. In most studies on MVD in ccRCC, the determination of MVD is performed manually by counting small caliber vessels that are identified by immunohistochemistry. Rules for reproducible manual microvessel counting were defined by Weidner [1]. However, the method by Weidner is prone to a high interobserver variability [13,18], and it depends on the experience of the pathologist and on poorly controlled variables, including the quality of different antibodies to detect endothelial cells.

Thus the technique used to determine tumor vascular density can affect the significance of the results. In the present study, we describe the evaluation of MVA as a novel parameter in ccRCC patients by the AQUA system. The fluorescence-based AQUA system is more objective, unbiased, and reproducible than manual biomarker evaluation. AQUA can be applied to standard slides and TMAs, allowing automated high-throughput quantification of biomarkers [21]. To facilitate automation in a high-throughput setting, we evaluated formalin-fixed, paraffin-embedded, archival specimens from 284 patients with primary ccRCCs arranged in TMAs. To the best of our knowledge, this is the largest sample cohort that is reported in the literature to be systematically evaluated for the degree of angiogenesis in ccRCC. We developed a computer-aided approach to determine MVA as a measurement of angiogenesis in primary ccRCCs by using an antibody against the endothelial marker CD34 and defined a ccRCC-specific epithelial/stromal mask with EMA, CD10, and vimentin. The results were compared with prognostic parameters of ccRCC (tumor grade, stage, size, metastasis, presence of necrosis, sarcomatoid features, lymphocytic infiltration, metastases, and cancer-specific survival). The AQUA approach allowed for fast, objective, straightforward, and highly reproducible measurement of tumor vascularity in a high-throughput setting.

AQUA is not as widely used as other image analysis systems. We preferred AQUA to alternative approaches because immunofluorescence as detected by the AQUA system is more sensitive than conventional immunohistochemistry (data not shown). By creating a ccRCC-specific epithelial/stromal mask, we were able to objectively quantify tumor-associated vessels. However, AQUA measures vessel areas and is therefore dependent on the vessel size, whereas manual MVD determination counts single microvessels and depends on the vessel number only. A large vessel would be counted as 1 vessel by the pathologist but AQUA would consider this a large MVA because of the thick vessel walls contributing to the vessel density. This accounts for differing results in a few cases for MVA as determined by AQUA and MVD manually counted according to Weidner. Surprisingly, a large MVA as determined by AQUA correlates with a high manually counted MVD. We were able to confirm an association between large areas of microvessels and better patient prognosis, a result that was also reported for manual quantification of MVD [11,12,14,15,18,29].

The reason why poorly vascularized ccRCC tumors are more often associated with worse clinical prognosis is not clear. In this respect, ccRCC differs from other solid malignancies. Certain hypotheses addressing this paradox have been attempted. Kohler et al [30] suggested that the decreased MVD in high-grade RCCs reflects the inability of tumor neovascularization to keep pace with the proliferation of the high-grade tumor cells, and increased tumor vessel permeability may compensate for their reduced amount. Herbst et al [12] considered the RCC microvasculature as a potential parameter of tumor differentiation. The renal tubular system is closely associated with a highly vascularized stroma, and inasmuch as RCC originates from the renal proximal tubular system, it is not surprising that a well-differentiated, low-grade RCC has an abundant vascular stroma. An additional mechanism explaining this paradox may be a modification of the vasculature in ccRCC during development, with high-grade/poor-prognosis tumors having a decreased vascular density. Delahunt et al [11] hypothesize that the development of large-diameter vascular channels in larger tumors could be the reason for decreasing MVD in such tumors. Quantifying MVA by AQUA provides an assessment of vessel numbers and is also dependent on the size of vessels in a given area of tumor. AQUA does not distinguish between tumors containing numerous small vessels and those with fewer, but larger, diameter vascular channels. Instead, the AQUA system provides an overall quantification of vessel areas within tumor tissue. Using this approach, we confirmed the findings of other groups and found a positive association between survival and MVA in ccRCC. Apparently, the development of large vessels within ccRCC tumors that may contribute to blood-borne metastatic spread results in a large MVA, but is not associated with poor prognosis.

Finally, this paradox has been suggested to be related to the architectural pattern of tumor growth of ccRCC, which is in contrast to the growth patterns of other tumors where MVD is strongly associated with aggressive behavior [15]. Breast carcinomas, for example, have an infiltrative pattern of growth, whereby tumor epithelial/host stromal interactions play a key role

in tumor progression. In these tumors, increased stromal angiogenesis will lead to a more rapidly infiltrating tumor. RCC typically grows as a well-demarcated bulging mass with a delicate vascular stroma. A well-vascularized RCC will continue to enlarge slowly as a mass lesion. A high-grade solid RCC enlarges more rapidly, overcoming its vascular network and decreasing its architectural complexity.

Our results suggest that computer-assisted image analysis of complex vascular architecture by AQUA is a rapid, reproducible, and objective alternative to the quantification of MVD by an experienced pathologist in a high-throughput setting. We were able to unequivocally correlate MVA with nuclear grade, tumor stage, metastatic behavior, the presence of sarcomatoid features, necrosis, and lymphocytic infiltration, thus identifying MVA as an important prognostic marker for ccRCC. MVA was found to be associated with cancer-specific death at the univariate level. In addition, we have defined and validated 2 cutoff points to categorize tumor MVA that may serve as a template profile for further analyses. From these results it can be anticipated that AQUA will become a generally applicable method for the quantification of MVA as a diagnostic parameter, also in other tumors.

Acknowledgments

We thank Xiao-Wei Sun for expert and diligent technical support.

References

[1] Weidner N. Intratumor microvessel density as a prognostic factor in cancer. Am J Pathol 1995;147:9-19.
[2] Obermair A, Kurz C, Czerwenka K, et al. Microvessel density and vessel invasion in lymph-node-negative breast cancer: effect on recurrence-free survival. Int J Cancer 1995;62:126-31.
[3] Brawer MK. Quantitative microvessel density. A staging and prognostic marker for human prostatic carcinoma. Cancer 1996;78: 345-9.
[4] Jaeger TM, Weidner N, Chew K, et al. Tumor angiogenesis correlates with lymph node metastases in invasive bladder cancer. J Urol 1995; 154:69-71.
[5] Vermeulen PB, Van den Eynden GG, Huget P, et al. Prospective study of intratumoral microvessel density, p53 expression and survival in colorectal cancer. Br J Cancer 1999;79:316-22.
[6] Maeda K, Chung YS, Takatsuka S, et al. Tumour angiogenesis and tumour cell proliferation as prognostic indicators in gastric carcinoma. Br J Cancer 1995;72:319-23.
[7] Hollingsworth HC, Kohn EC, Steinberg SM, Rothenberg ML, Merino MJ. Tumor angiogenesis in advanced stage ovarian carcinoma. Am J Pathol 1995;147:33-41.
[8] Fallowfield ME, Cook MG. The vascularity of primary cutaneous melanoma. J Pathol 1991;164:241-4.
[9] Joo HJ, Oh DK, Kim YS, Lee KB, Kim SJ. Increased expression of caveolin-1 and microvessel density correlates with metastasis and poor prognosis in clear cell renal cell carcinoma. BJU Int 2004; 93:291-6.
[10] Fukata S, Inoue K, Kamada M, et al. Levels of angiogenesis and expression of angiogenesis-related genes are prognostic for organ-specific metastasis of renal cell carcinoma. Cancer 2005;103: 931-42.
[11] Delahunt B, Bethwaite PB, Thornton A. Prognostic significance of microscopic vascularity for clear cell renal cell carcinoma. Br J Urol 1997;80:401-4.
[12] Herbst C, Kosmehl H, Stiller KJ, et al. Evaluation of microvessel density by computerised image analysis in human renal cell carcinoma. Correlation to pT category, nuclear grade, proliferative activity and occurrence of metastasis. J Cancer Res Clin Oncol 1998;124:141-7.
[13] Paradis V, Lagha NB, Zeimoura L, et al. Expression of vascular endothelial growth factor in renal cell carcinomas. Virchows Arch 2000;436:351-6.
[14] Rioux-Leclercq N, Epstein JI, Bansard JY, et al. Clinical significance of cell proliferation, microvessel density, and CD44 adhesion molecule expression in renal cell carcinoma. Hum Pathol 2001; 32:1209-15.
[15] Sabo E, Boltenko A, Sova Y, Stein A, Kleinhaus S, Resnick MB. Microscopic analysis and significance of vascular architectural complexity in renal cell carcinoma. Clin Cancer Res 2001;7:533-7.
[16] MacLennan GT, Bostwick DG. Microvessel density in renal cell carcinoma: lack of prognostic significance. Urology 1995;46: 27-30.
[17] Slaton JW, Inoue K, Perrotte P, et al. Expression levels of genes that regulate metastasis and angiogenesis correlate with advanced pathological stage of renal cell carcinoma. Am J Pathol 2001;158: 735-43.
[18] Imao T, Egawa M, Takashima H, Koshida K, Namiki M. Inverse correlation of microvessel density with metastasis and prognosis in renal cell carcinoma. Int J Urol 2004;11:948-53.
[19] Camp RL, Chung GG, Rimm DL. Automated subcellular localization and quantification of protein expression in tissue microarrays. Nat Med 2002;8:1323-7.
[20] Camp RL, Dolled-Filhart M, King BL, Rimm DL. Quantitative analysis of breast cancer tissue microarrays shows that both high and normal levels of HER2 expression are associated with poor outcome. Cancer Res 2003;63:1445-8.
[21] Rubin MA, Zerkowski MP, Camp RL, et al. Quantitative determination of expression of the prostate cancer protein alpha-methylacyl-CoA racemase using automated quantitative analysis (AQUA): a novel paradigm for automated and continuous biomarker measurements. Am J Pathol 2004;164:831-40.
[22] Moch H, Schraml P, Bubendorf L, et al. High-throughput tissue microarray analysis to evaluate genes uncovered by cDNA microarray screening in renal cell carcinoma. Am J Pathol 1999;154:981-6.
[23] Eble JN, Sauter G, Epstein JI, Sesterhenn IA. World Health Organization classification of tumours. Pathology and genetics of tumours of the male urinary system and male genital organs. Journal 2004;1.
[24] Fina L, Molgaard HV, Robertson D, et al. Expression of the CD34 gene in vascular endothelial cells. Blood 1990;75:2417-26.
[25] Avery AK, Beckstead J, Renshaw AA, Corless CL. Use of antibodies to RCC and CD10 in the differential diagnosis of renal neoplasms. Am J Surg Pathol 2000;24:203-10.
[26] Fleming S, Lindop GB, Gibson AA. The distribution of epithelial membrane antigen in the kidney and its tumours. Histopathology 1985;9:729-39.
[27] Denekamp J, Hobson B. Endothelial-cell proliferation in experimental tumours. Br J Cancer 1982;46:711-20.

[28] Liotta LA, Kleinerman J, Saidel GM. Quantitative relationships of intravascular tumor cells, tumor vessels, and pulmonary metastases following tumor implantation. Cancer Res 1974;34:997-1004.
[29] Schraml P, Struckmann K, Hatz F, et al. VHL mutations and their correlation with tumour cell proliferation, microvessel density, and patient prognosis in clear cell renal cell carcinoma. J Pathol 2002;196:186-93.
[30] Kohler HH, Barth PJ, Siebel A, Gerharz EW, Bittinger A. Quantitative assessment of vascular surface density in renal cell carcinoma. Br J Urol 1996;77:650-4.